Influence of Fe_2O_3 on synthesis, physical, optical, and radiation shielding properties of $Na_2B_4O_7$-SiO_2-CaO-Fe_2O_3 glasses for radiation applications

D. A. Aloraini[a], Kh. S. Shaaban[b,*]

[a]*Department of Physics, College of Science, Princess Nourah bint Abdulrahman University, P.O. Box 84428, Riyadh, 11671, Saudi Arabia*

[b]*Department of Chemistry, College of Science, Al-Azhar University, P.O. 71524, Assiut, Egypt*

This work explored the optical properties and radiation resistance of $Na_2B_4O_7$-SiO_2-CaO-Fe_2O_3 glasses. As the Fe_2O_3 increase, the (ρ) increases from 2.37 for BSFe-0 to 3.43 g/cm³ for BSFe-2 while (V_m) decline from 69.80 cm³/mol for BSFe-0 to 48.83 cm³/mol for BSFe-2. The E_{opt} values obtained are 2.49, 2.34, 2.32, 2.21, and 2.19 eV for the BSFe-0, BSFe-0.5, BSFe-1, BSFe-1.5, and BSFe-2 glasses. With the addition of Fe_2O_3 to the base glasses at the expense of CaO, the Z_{eff} values increase. The trend in (Z_{eff}) values for BSFe glasses follows the order: BSFe-2 > BSFe-1.5 > BSFe-1 > BSFe-0.5 > BSFe-0. This indicates that higher Z_{eff} values are because of the existence of Fe_2O_3. Accordingly, BSFe-2 glass samples with the higher content of Fe_2O_3, exhibits greater photon interaction with $\gamma -$ radiation. As a result, BSFe-2 is more suitable for γ and neutron shielding application compared to the other samples.

(Received January 3, 2025; Accepted March 31, 2025)

Keywords: Fe_2O_3, optical, γ, Neutron

1. Introduction

Glasses based on the transition metal oxides (TMOs) demonstration exclusive features that make them greatly valuable for various applications [1-5]. Altering the kind and content of (TMOs) in the glass matrix allows for fine adjustment of their refractive index, absorption, and bandgap ($E_{opt.}$). This tunability is valuable for constructing custom optical components. TMOs donate to powerful nonlinear optical effects, which are advantageous in photonic applications such as frequency conversion, optical switching, and the growth of ultrafast lasers. Glasses, including TMOs, generally display acceptable thermal stability and resistance to chemical degradation, making them reliable for use in harsh conditions [6-8]. Particular, TMO-based glasses such as Fe_2O_3 exhibit semiconducting properties, making them valuable in electronic and photovoltaic devices [9-11].

Borosilicate glasses (BSGs) are known for their remarkable properties, making them is greatly suitable for numerous technical applications. (BSGs) are highly resistant to chemical corrosion, including acids, bases, and water. This property is critical for containers used in chemical processing, pharmaceuticals, and food storage. BSGs are non-toxic and biocompatible, permitting their use in medical applications such as implants, vials, and syringes. BSGs are resistant to radiation-induced, making them beneficial for optical components in nuclear establishments [16-21]. Investigators are analyzing the possibility of glass materials for radiation shielding, as advancements in glass technology expand its applications [16-21].

Fe_2O_3 is a compelling choice to CaO in glass systems for radiation shielding, especially for the following reasons: Fe_2O_3 has a higher density (5.25g/cm^3) compared to CaO (3.34 g/cm^3), which improve its ability to attenuate the energy of incoming photons. The Z of Fe (26) is remarkably greater than Ca (Z= 20), which improve the interaction possibility with high-energy photons. Fe_2O_3 is therefore, a better option for X-ray and γ-ray shielding. The Fe_2O_3 in the BSGs

* Corresponding author: khamies1078@yahoo.com
https://doi.org/10.15251/DJNB.2025.201.373

might shield spacecraft from cosmic radiation. The incorporation of Fe_2O_3 in the BSGs increases the MAC, enhancing the glass's ability to block or reduce radiation. Thus, these glasses can be used with radiology equipment and X-ray rooms.

This work examines how the glass system's optical characteristics alter when CaO and Fe_2O_3 are exchanged. Furthermore, evaluating these glasses' suitability as radiation-shielding materials requires examining how they react to gamma and neutron irradiation. By analyzing the optical characteristics and irradiation response, we can assess the effectiveness and possible uses of these glasses as radiation-shielding glasses.

2. Materials and methods

Fig. 1 presented the fabrication procedure and photographs of BSFe samples. The (ρ) was measured using the Archimedes technique, and molar volume (V_m) was considered.

$$\rho = \rho_0 \left(\frac{W_a}{W_a - W_b}\right) \tag{1}$$

$$V_m = M/\rho, \tag{2}$$

Ion concentration: $N_i = \left(\frac{6.023\times10^{23} x\ mol\ fraction\ of\ cation \times valency\ of\ cation}{Vm}\right),$ (3)

Polaron radius: $r_p = \frac{1}{2}\left(\frac{\pi}{6N}\right)^{\frac{1}{3}},$ (4)

Inter-nuclear distance $(r_i) = \left(\frac{1}{N}\right)^{\frac{1}{3}},$ (5)

Separation of $(d_{Cd-Cd}) = \left(\frac{V_m^B}{N}\right)^{\frac{1}{3}}$ (6)

Field strength: $F = (Pbi/r_p^2)$ (7)

The optical spectra were detailed by a double- beam spectrophotometer (Unicam, England). The radiation parameters can be evaluated for BSFe glasses with the Phy-X [22] code.

3. Results and discussion

3.1. Physical exploration

Fig. 2 exemplifies the (ρ g/cm³) and (V_m) of BSFe glasses. As the Fe_2O_3 increase, the (ρ) increases from 2.37 for BSFe-0 to 3.43 for BSFe-2. This increase is attributed to the higher molar mass of Fe_2O_3 (159.69) compared to CaO (56.077). Accordingly, the addition of Fe_2O_3 to the base glasses significantly enhances the (ρ). The (V_m) decline from 69.80 cm³/mol for BSFe-0 to 48.83 cm³/mol for BSFe-2. This inverse relationship between (ρ) and (V_m) is well-documented [23-25]

As the content of Fe_2O_3 increases the r_p, r_i, and (d_{Cd-Cd}) values decrease. The (ρ) and (V_m) values have confirmed these results. The values of $(N_i\ and\ F)$ are increased due to the rise in the Fe_2O_3content. Table 1 recorded these data.

Table 1. Physical data.

Code	BSFe-0	BSFe-0.5	BSFe-1	BSFe-1	BSFe-2
N_i*10^20^	-	0.47	1.06	1.74	2.47
r_p	-	32.21	24.63	20.90	18.64
r_i	-	9.25	7.07	6.00	5.35
d_{Cd-Cd}	0.695	0.675	0.649	0.630	0.617
F	-	0.023	0.04	0.06	0.07

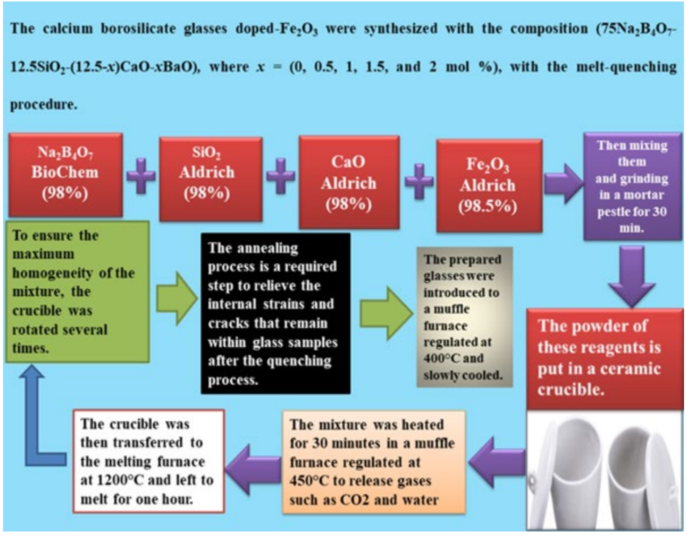

Fig. 1. The manufactured of glasses.

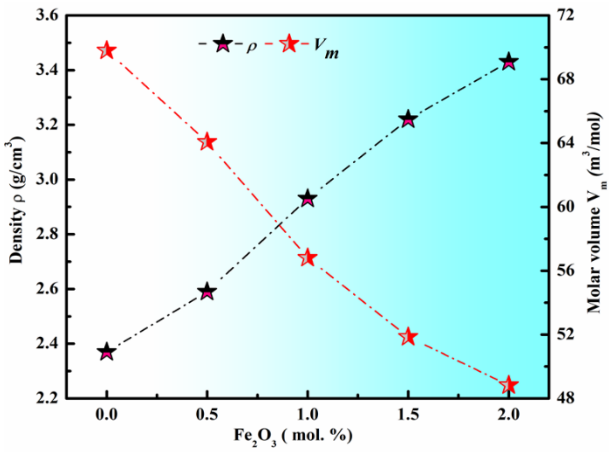

Fig. 2. (ρ) and (V_m), of the BSFe glasses.

3.2. Optical characteristics

The optical characteristics of glasses typically determine their use in different applications [26-30]. This investigation shows that the transparent colour of glass samples without Fe_2O_3 turns light brown when Fe_2O_3 is added, and then turns darker brown as Fe_2O_3 additives are increased as Fig. 1b. This brown hue supports the presence of Fe^{2+} ions as FeO6 in the current BSFe glasses based on Weyl's classification system for coloured glasses [31]. Additionally, the fact that the glass is brown shows that the Fe^{3+} cations are not responsible for the coloration. The presence of Fe^{+2} in the FeO6 configuration acts as glass modifiers and creating (NBOs) within the glass network. Furthermore, the increased brown colour observed with varying concentrations of Fe_2O_3 (see Fig. 1b) indicates the conversion of Fe^{3+} to Fe^{2+} with additional Fe_2O_3 at the expense of CaO.

In the UV-vis-NIR (200 to 2600 nm), the absorption spectra of BSFe-glass with different Fe_2O_3 additions were analyzed. The absorption spectra coefficient (α) are shown in Fig. 3.

$$\alpha = \frac{2.303}{d}\,(A) \tag{8}$$

(α) can be used for calculated the bandgap energy (E_{opt}) for BSFe glasses as [32-36]: $\alpha . h\nu = C(h\nu - E_{opt})^{1/2}$ (9)

The E_{opt} predicted by plotting the ($h\nu$) against ($\alpha h\nu$) $^{0.5}$ as Fig. 4. Fig. 5 shows the changes in E_{opt} for BSFe-glasses about Fe_2O_3 contents (mol %).The E_{opt} values obtained are 2.49, 2.34, 2.32, 2.21, and 2.19 eV for the BSFe-0, BSFe-0.5, BSFe-1, BSFe-1.5, and BSFe-2 glasses. Fig. 5 shows that the E_{opt} decline from 2.49 to 2.19 e.V. This decrease could be explained by the bonds in the glass network having a higher ionic character and a lower covalent character. This decrease is also caused by the replacement of (Λ, CaO = 1) with (Λ, Fe_2O_3 = 1.04) [37].

An important consideration when assessing the optical characteristics of glass samples is the refractive index (n), which is expressed as follows:

$$n = \frac{(1-R)^2 + k^2}{(1+R)^2 + k^2} \quad (10)$$

where R is reflectance. (R) is displayed in Fig. 6. The R values increase. The BSFe samples (n) are expressed as a function of (λ) in Fig. 7. An increase in Fe_2O_3 typically increases (n). As the Fe_2O_3 content of BSFe glasses increases, the glass's density rises, this causes the refractive index to rise as well. The values of (n) and (ρ) in the glasses have a linear relationship.

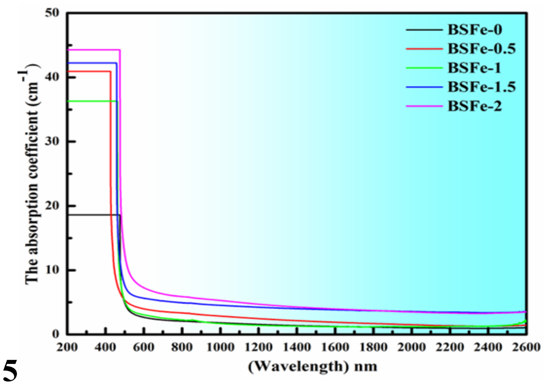

5

Fig. 3. α of BSFe glasses.

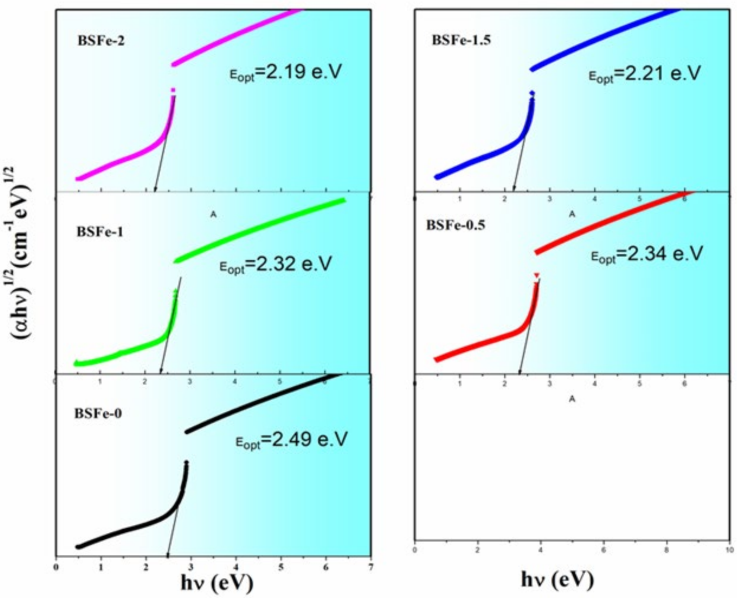

Fig. 4. (hν) against (αhν) $^{0.5}$ to estimate the (E_{opt}) for BSFe glasses.

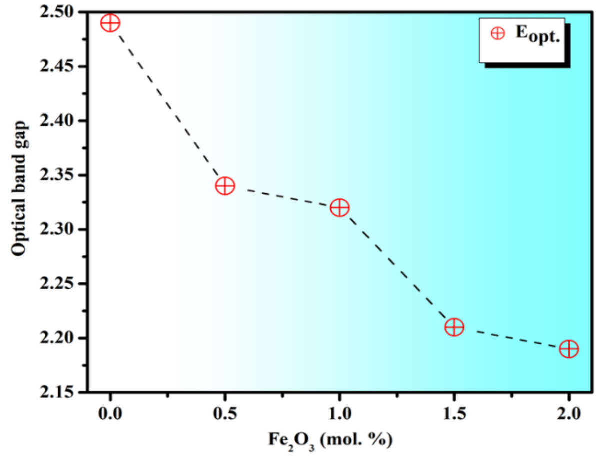

Fig. 5. (E_{opt}) against Fe_2O_3 content for BSFe glasses.

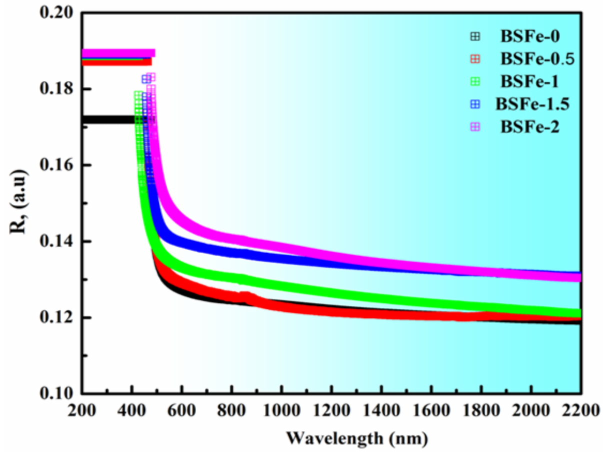

Fig. 6. (R) of BSFe glasses.

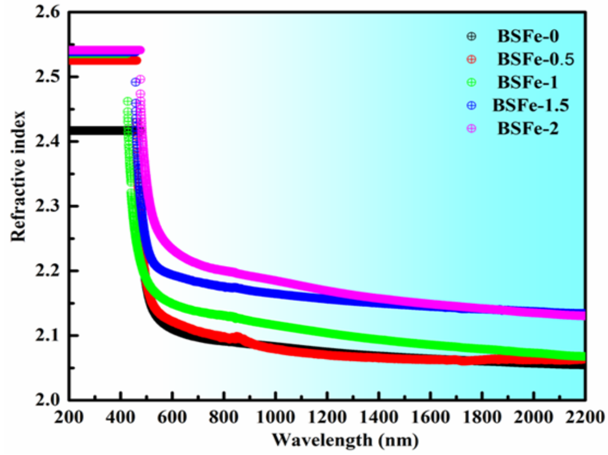

Fig. 7. (n) of BSFe glasses.

3.3. Gamma radiation shielding properties

The attractive force that an atom's outermost electrons experience is measured by its effective atomic number, Z_{eff} and can be expressed as [38-47]:

$$Z_{eff} = \frac{\sum_i F_i A_i (\mu/\rho) i}{\sum_i F_i \frac{A_i}{Z_i} (\mu/\rho) i} \quad (11)$$

The relationship between photon energy (E) and the (Z_{eff}) is displayed in Fig. 8. As the (E) rises, the (Z_{eff}) values progressively fall. The (Z_{eff}) values of BSFe glasses decrements from 10.88055 to 8.05217 for BSFe-0, 11.19783 to 8.07431 for BSFe-0.5, 11.50298 to 8.09636 for BSFe-1, 11.79669 to 8.11833 for BSFe-1.5, and from 12.07959 to 8.14022 for BSFe-2, at (E) ranged (0.015-15 MeV). With the addition of Fe_2O_3 to the base glasses at the expense of CaO, the Z_{eff} values increase. This increment can be related to the higher Z of Fe_2O_3 (26) compared to CaO (20) [57–64]. The trend in (Z_{eff}) values for BSFe glasses follows the order: BSFe-2 > BSFe-1.5 > BSFe-1 > BSFe-0.5 > BSFe-0. Additionally, the study discovered that Z_{eff} values rise as Fe_2O_3 levels rise. This indicates that higher Z_{eff} values are because of the existence of Fe_2O_3. Accordingly, BSFe-2 glass samples with the higher content of Fe_2O_3, exhibits greater photon interaction with $\gamma -$ radiation [38–47]. As a result, BSFe-2 is more suitable for shielding application compared to the other samples.

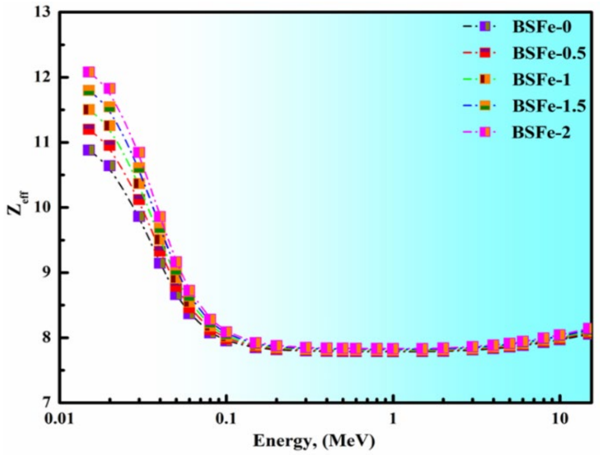

Fig. 8. Z_{eff} of BSFe glasses.

3.4. Neutron radiation shielding properties

The calculation of fast neutron attenuation is based on the fast neutron removal cross-section (∑R), (FNRC, cm^{-1}), and considered as:

$$\left(\frac{\Sigma_R}{\rho}\right) = \sum_i w_i \left(\frac{\Sigma_R}{\rho}\right)_i \quad (12)$$

$$R = \sum_i \rho_i \left(\frac{R}{\rho}\right)_i \quad (13)$$

The ∑R is shown in Fig. 9. The ∑R values of BSFe glasses increments from 0.099 for BSFe-0, 0.108 for BSFe-0.5, 0.122 for BSFe-1, 0.134 for BSFe-1.5, and to 0.143 for BSFe-2. With the addition of Fe_2O_3 to the base glasses at the expense of CaO, the ∑R values increase. The trend in ∑R values for BSFe glasses follows the order: BSFe-2 > BSFe-1.5 > BSFe-1 > BSFe-0.5 > BSFe-0. This increment can be related to the greater (ρ) of the samples with the addition of Fe_2O_3. This indicates that higher ∑R values are because of the existence of Fe_2O_3. Accordingly, BSFe-2 glass samples with the higher content of Fe_2O_3, exhibits greater neutron radiation [38–47]. As a result, BSFe-2 is more suitable for neutron shielding application compared to the other samples.

The BSFe glasses and the materials commonly used for neutron attenuation are compared in Fig. 9. BSFe samples have higher ∑R values than those of several known neutron materials attenuation, such as concert (0.094), H_2O (0.102), barite (0.10126), graphite (0.077), Rs-253-G18 (0.08632), RS-360 (0.06515), and RS-520 (0.07743). The present glasses have higher $\sum R$ values than those materials, suggesting that they could be used as neutron attenuation enhancements in a variety of applications.

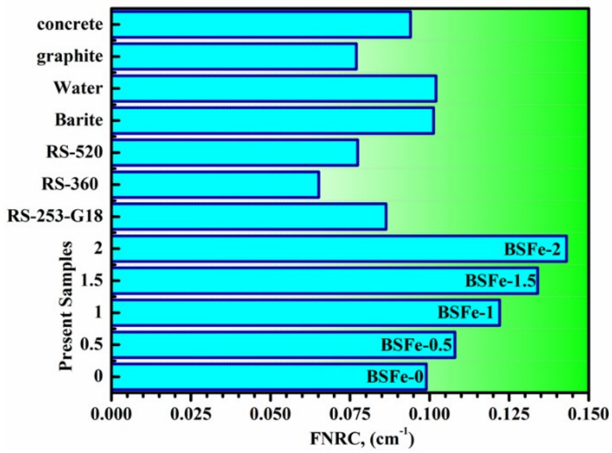

Fig. 9. FNRC of BSFe glasses.

5. Conclusions

Five glasses were successfully fabricated utilizing a fast melt-quenching approach. The glass configuration is $75Na_2B_4O_7$–$12.5SiO_2$–$(12.5\text{-}x)CaO$–xFe_2O_3, $x =$ $(0 \leq x \geq 2)$. This investigation shows that the transparent colour of glass samples without Fe_2O_3 turns light brown when Fe_2O_3 is added, and then turns darker brown as Fe_2O_3 additives are increased. Furthermore, the increased brown colour observed with varying concentrations of Fe_2O_3 indicates the conversion of Fe^{3+} to Fe^{2+} with additional Fe_2O_3 at the expense of CaO. As the Fe_2O_3 increase, the (ρ) increases from 2.37 for BSFe-0 to 3.43 g/cm³ for BSFe-2 while the (V_m) decline from 69.80 cm³/mol for BSFe-0 to 48.83 cm³/mol for BSFe-2. The E_{opt}values obtained are 2.49, 2.34, 2.32, 2.21, and 2.19 eV for the BSFe-0, BSFe-0.5, BSFe-1, BSFe-1.5, and BSFe-2 glasses.

The E_{opt} values decline from (2.49 to 2.19 e.V) with a rise in the Fe_2O_3. With the incorporation of Fe_2O_3 to the base glasses at the expense of CaO, the Z_{eff} values increase. The trend in (Z_{eff}) values for BSFe glasses follows the order: BSFe-2 > BSFe-1.5 > BSFe-1 > BSFe-0.5 > BSFe-0. This indicates that higher Z_{eff} values are because of the existence of Fe_2O_3. Accordingly, BSFe-2 sample with the greater content of Fe_2O_3 exhibits greater photon interaction with $\gamma -$ radiation. As a result, BSFe-2 is more suitable for γ and neutron shielding application compared to the other samples.

Acknowledgments

The authors express their gratitude to Princess Nourah bint Abdulrahman University Researchers Supporting Project number (PNURSP2025R57), Princess Nourah bint Abdulrahman University, Riyadh, Saudi Arabia.

References

[1] Sayyed M.I., Sadeq M.S., Shaaban, K.S., Abd El-Rehim A.F., Atif Mossad Ali, H.Y. Morshidy, Optical Materials, **142**, 114051, (2023); https://doi.org/10.1016/j.optmat.2023.114051.
[2] Shaaban, K.S., Alyousef, H.A. & El-Rehim, A.F.A., Silicon **14**, 12001, (2022); https://doi.org/10.1007/s12633-022-02124-5
[3] Shaaban, K.S., Alotaibi, B.M., Alharbiy, N. et al. Silicon **14**, 11991, (2022); https://doi.org/10.1007/s12633-022-02029-3
[4] Wahab, E.A.A., Shaaban, K.S., Al-Baradi, A.M., Silicon **14**, 4915, (2022); https://doi.org/10.1007/s12633-021-01236-8
[5] Almutairi, H.M., Aloraini, D.A., Alsafi, K. Al-Saleh W. M., Alzahrani A. S., Shaaban, K. S., Silicon **16**, 2873, (2024); https://doi.org/10.1007/s12633-024-02900-5
[6] Shaaban, K.S., Al-Baradi, A.M., Ali, A.M. Silicon **14**, 10375, (2022); https://doi.org/10.1007/s12633-022-01783-8
[7] Althagafi, T.M., Sayed, M.A., Alghasham, H.A. Nuha Al-Harbi, Kh. S. Shaaban, Silicon **15**, 7047, (2023); https://doi.org/10.1007/s12633-023-02567-4
[8] Aloraini, D.A., Ashour, A., Shaaban, K.S. Silicon **16**, 1837, (2024); https://doi.org/10.1007/s12633-023-02804-w
[9] Alomairy, S., Aboraia, A.M., Shaaban, E.R., Shaaban, K.S., Brazilian Journal of Physics 51, 1237, (2021); https://doi:10.1007/s13538-021-00928-1
[10] Shaaban, Kh. S., Al-Baradi, Ateyyah M. and Aloraini, Dalal Abdullah., Radiochimica Acta, (2025); https://doi.org/10.1515/ract-2024-0356
[11] Basha B., Shaaban, K.S., Abdel Wahab E.A., Digest Journal of Nanomaterials and Biostructures 18, (2), 713, (2023); https://doi.org/10.15251/DJNB.2023.182.713
[12] Shaaban, K.S., Al-Baradi, A.M., Ali, A.M., Silicon **14**, 8971, (2022); https://doi.org/10.1007/s12633-022-01702-x
[13] Sayed, M.A., Basha, B., Al-Harbi, N. Shaaban, K. S., Silicon, **15**, 6463, (2023); https://doi.org/10.1007/s12633-023-02537-w
[14] Shaaban, K. S., Al-Baradi, A. M., Alotaibi, B., El-Rehim, A., Journal of Materials Research and Technology, **23**, 756, (2023); https://doi.org/10.1016/j.jmrt.2023.01.062
[15] Shaaban, K. S., Al-Baradi, A. M., Ali, A. M. RSC Advances, 12 (5), 3036, (2022); https://doi.org/10.1039/D2RA00171C
[16] Shaaban, K., Alotaibi, B., Alharbi, N., Alrowaili, Z., Al-Buriahi, M., Makhlouf, S. A., Abd El-Rehim, A., Radiation Physics and Chemistry, **193**, 109995, (2022); https://doi.org/10.1016/j.radphyschem.2022.109995
[17] Shaaban, K.S., Al-Baradi, A.M., Ali, A.M. P J Mater Sci: Mater Electron **33**, 3297, (2022); https://doi.org/10.1007/s10854-021-07530-w
[18] Sayed, M.A., Ali, A.M., Abd El-Rehim, A.F. Wahab, E.A.A., Shaaban, K.S. J. Electron. Mater **50**, 3116, (2021); https://doi.org/10.1007/s11664-021-08921-9
[19]Shaaban, K.S., Wahab, E.A.A., Shaaban, E.R. et al., Opt Quant Electron **52**, 125, (2020); https://doi.org/10.1007/s11082-020-2191-3
[20] Alghasham, H. A., Ismail, Y. A., Aloraini, D. A., Shaaban, K., Materials Today Communications, **38**, 107840, (2024); https://doi.org/10.1016/j.mtcomm.2023.107840
[21] El-Rehim, A.F.A., Zahran, H.Y., Yahia, I.S. Atif Mossad Ali, Shaaban, K.S. Silicon **14**, 405, (2022); https://doi.org/10.1007/s12633-020-00827-1
[22] Şakar E, Özpolat ÖF, Alım B, Sayyed MI, Kurudirek M, Radiation Phys Chem **166**: 108496, (2020); https://doi.org/10.1016/j.radphyschem
[23] Shaaban, K.S., Al-Baradi, A.M., Wahab, E.A.A, Silicon, **14**, 5057, (2022); https://doi.org/10.1007/s12633-021-01309-8
[24] Al-Baradi, A.M., Wahab, E.A.A., Shaaban, K.S. Silicon **14**, 5277, (2022); https://doi.org/10.1007/s12633-021-01286-y
[25] Shaaban, K.S., Alotaibi, B.M., Al-Baradi, A.M. Yousef El Sayed, Ashour A., Silicon **15**, 4409, (2023); https://doi.org/10.1007/s12633-023-02351-4

[26] Alsafi, K., Ismail, Y. A., Aloraini, D. A., Issa, S. A., Abdel Wahab, E., Shaaban, K. S. Radiation Physics and Chemistry, **220**, 111707. (2024); https://doi.org/10.1016/j.radphyschem.2024.111707
[27] Alotaibi, B., Alhuzaymi, T. M., Alotiby, M. F., Makhlouf, S. A., Shaaban, K., Abdel Wahab, E. Optik, **301**, 171689, (2024); https://doi.org/10.1016/j.ijleo.2024.171689
[28] Shaaban, K.S., Alomairy, S., Al-Buriahi, M.S. J Mater Sci: Mater Electron **32**, 26034, (2021); https://doi.org/10.1007/s10854-021-05885-8
[29] Shaaban, K. S., Tamam, N., Alghasham, H. A., Alrowaili, Z., Al-Buriahi, M., Ellakwa, T. E. Materials Today Communications, **37**, 107325, (2023); https://doi.org/10.1016/j.mtcomm.2023.107325
[30] Mahrous, Eman M., Al-Baradi, Ateyyah M. and Shaaban, Kh. S., Radiochimica Acta, (2024); https://doi.org/10.1515/ract-2024-0307
[31] W.A. Weyl, Coloured Glasses, Society of Glass Technology, Sheffield, UK (1999);
[32] Wahab, E.A.A., Alyousef, H.A., El-Rehim, A.F.A. et al., J. Electron. Mater. **52**, 219, (2023); https://doi.org/10.1007/s11664-022-09969-x
[33] Shaaban, K.S., Alotaibi, B.M., Yousef, E.S. J. Electron. Mater. **52**, 3591, (2023); https://doi.org/10.1007/s11664-023-10347-4
[34] Al-Baradi, A.M., Alotaibi, B.M., Alharbi, N. A.F. Abd El-Rehim, Shaaban, K.S, Silicon **14**, 10391, (2022); https://doi.org/10.1007/s12633-022-01801-9
[35] Shaaban, K.S., Alsafi, K., Aloraini, D.A. Wafa M. Al-Saleh, Haifa M. Almutairi, E. E. Assem. Silicon **16**, 2899, (2024); https://doi.org/10.1007/s12633-024-02897-x
[36] El-Rehim, A.F.A., Zahran, H.Y., Yahia, I.S., Wahab, E.A.A., Shaaban, K.S., Journal of Materials Engineering and Performance 30, 1872, (2021); https://doi:10.1007/s11665-021-05513-w
[37] Dimitrov, V., Komatsu, T. Journal of Solid State Chemistry, 163(1), 100-112. (2001); https://doi.org/10.1006/jssc.2001.9378
[38] Shaaban, K.S., Alrowaili, Z.A., Al-Baradi, A.M. Atif Mossad Ali, E. A. Abdel Wahab, M. S. Al-Buriahi. Silicon **14**, 6457, (2022); https://doi.org/10.1007/s12633-021-01441-5
[39] Almutairi, H.M., Aloraini, D.A., Alsafi, K. Al-Saleh W. M., Alzahrani A. S., Shaaban, K. S. Silicon **16**, 2873, (2024); https://doi.org/10.1007/s12633-024-02900-5
[40] Shaaban, K. S., Aloraini, D. A., Alsafi, K., Almutairi, H. M., Al-Saleh, W. M., Alzahrani, A. S. Materials Today Communications, **38**, 108309, (2024); https://doi.org/10.1016/j.mtcomm.2024.108309
[41] Shaaban, K. S., Al-Harbi, N., Alyousef, H. A., Al-Baradi, A. M., Ali, A. M., Abdel Wahab, E. Radiation Physics and Chemistry, **212**, 111086, (2023); https://doi.org/10.1016/j.radphyschem.2023.111086
[42] Alsafi, K., Ismail, Y. A., Aloraini, D. A., Almutairi, H. M., Al-Saleh, W. M., Shaaban, K. S. Progress in Nuclear Energy, **170**, 105151, (2024); https://doi.org/10.1016/j.pnucene.2024.105151
[43] Shaaban, K. S., Althagafi, T. M., Ashour, A., Alalawi, A., Al-Buriahi, M., Ibraheem, A. A. Radiation Physics and Chemistry, **216**, 111440, (2024); https://doi.org/10.1016/j.radphyschem.2023.111440
[44] Alsafi, Khalid, Aloraini, Dalal Abdullah, Saif, M. A., Shaaban, Kh. S., Radiochimica Acta, (2024); https://doi.org/10.1515/ract-2024-0272
[45] B. M. Alotaibi, Thaqal M. Alhuzaymi, Mohammed. F. Alotiby, Sayed. A. Makhlouf, Kh. S. Shaaban, E. A. Abdel Wahab, Chalcogenide letters, **21**(8), 583, (2024);
[46] Mahrous, E.M., Al-Baradi, A.M., Shaaban, K.S., Radiochimica Acta, (2024); https://doi.org/10.1515/ract-2024-0307
[47] Shaaban, K. S., Aloraini, D. A. Materials Research Bulletin, 184, 113266. (2025); https://doi.org/10.1016/j.materresbull.2024.113266